UCRL-JRNL-228381

LAWRENCE
LIVERMORE
NATIONAL
LABORATORY

Modeled tephra ages from lake sediments, base of Redoubt Volcano, Alaska

C. J. Schiff, D. S. Kaufman, K. L. Wallace, A. Werner, T. L. Ku, T. A. Brown

February 27, 2007

Quaternary Geochronology

Modeled tephra ages from lake sediments, base of Redoubt Volcano, Alaska

Caleb J. Schiff[a], Darrell S. Kaufman[a*], Kristi L. Wallace[b], Al Werner[c], Teh-Lung Ku[d], Thomas A. Brown[e]

[a] *Department of Geology, Northern Arizona University, Flagstaff, AZ 86011-4099, USA*

[b] *U.S. Geological Survey, Alaska Volcano Observatory, Anchorage, AK 99508, USA*

[c] *Department of Earth and Environment, Mt. Holyoke College, South Hadley, MA 01075, USA*

[d] *Department of Earth Science, University of Southern California, Los Angeles, CA 90089, USA*

[e] *Center for Accelerator Mass Spectrometry, Lawrence Livermore National Laboratory, Livermore, CA 94551, USA*

*Corresponding author. Tel.: + 1 928 523 7192.

Email address: Darrell.Kaufman@nau.edu

Abstract

A 5.6-m-long lake sediment core from Bear Lake, Alaska, located 22 km southeast of Redoubt Volcano, contains 67 tephra layers deposited over the last 8750 cal yr, comprising 15% of the total thickness of recovered sediment. Using 12 AMS ^{14}C ages, along with the ^{137}Cs and ^{210}Pb activities of recent sediment, we evaluated different models to determine the age-depth relation of sediment, and to determine the age of each tephra deposit. The age model is based on a cubic smooth spline function that was passed through the adjusted tephra-free depth of each dated layer. The estimated age uncertainty of the 67 tephras averages ± 105 yr (1σ). Tephra-fall frequency at Bear Lake was among the highest during the past 500 yr, with eight tephras deposited compared to an average of 3.7 per 500 yr over the last 8500 yr. Other periods of increased tephra fall occurred 2500-3500, 4500-5000, and 7000-7500 cal yr. Our record suggests that Bear Lake experienced extended periods (1000-2000 yr) of increased tephra fall separated by shorter periods (500-1000 yr) of apparent quiescence. The Bear Lake sediment core affords the most comprehensive tephrochronology from the base of the Redoubt Volcano to date, with an average tephra-fall frequency of once every 130 yr.

Keywords: tephrochronology, Redoubt Volcano; tephra; Cook Inlet; volcanic hazards; tephra-fall frequency; Alaska

1. Introduction

Lakes are key geologic archives because, unlike other terrestrial depositional settings, sediment accumulates continuously in lakes and the preservation potential of deposits is high. Late Quaternary lake sediment can usually be dated by radiometric methods such as ^{14}C and ^{210}Pb. In volcanically active regions, lake sediment preserves tephra from nearby volcanoes and, combined with an age-depth model, can provide valuable records of late Quaternary eruption and tephra-fall frequency. Acquiring a well-dated tephrochronology from lake sediment is challenging, however. Holocene tephras are generally too young for direct dating by the decay of long-lived radioisotopes (e.g., K-Ar). Radiocarbon ages on organic matter directly below or within a tephra bed provide the most useful information for determining the timing of each tephra fall. Bioturbation, hardwater effects, or the input of organic matter to the lake following long-term storage on the landscape can lead to aberrant ^{14}C ages, however. Moreover, dating each tephra in lake sediment can be impractical because organic matter suitable for ^{14}C analysis rarely occurs adjacent to each tephra layer, and some lakes contain too many tephra layers to be cost effective (e.g., >100 at Paradox Lake, Kenai Peninsula; de Fontaine et al., in press). Therefore, the most practical approach to obtaining accurate ages for an entire sequence of tephras within a sediment core is to develop an age-depth model based on interpolation between dated levels (e.g., Andrews et al., 1999).

The type of interpolation best suited for age-depth modeling of sediment cores has been considered in previous studies (e.g., Bennett, 1994; Boreux et al., 1997; Telford et al., 2004a). Because of the uncertainties inherent in radiometric dating and those associated with the age of the dated sample relative to the surrounding sediment, any single age is unlikely to be absolutely correct. Smoothing functions can minimize these errors by relying on the assumption that changes in sedimentation rate occur relatively slowly and uniformly, rather than imposing stepped rate changes at the level at each dated sample. This seems reasonable in absence of lithostratigraphic or chronologic evidence for abrupt change (e.g., slump deposits, age reversals, and erosive contacts). In lakes with little fluvial input, a significant tephra fall event causes a rapid increase in sedimentation rate compared to the background sedimentation within the lake. Where tephra layers comprise a significant proportion of the total lake sediment, they must be accounted for when determining core chronology.

In this study, we evaluate several functions for modeling the age-depth relation as applied to a lake core from Bear Lake near Redoubt Volcano, Alaska. A previous core from this lake (Riehle, 1985) demonstrated that numerous tephra layers were preserved in the lake deposits. At the time of the previous study, however, AMS dating was not routinely available and few radiocarbon ages were obtained. We then use the new age model to derive the ages of each tephra bed preserved within the lake deposits. This record provides new insight into the tephra-fall frequency for south-central Alaska. Our study extends the historical eruptive record (since AD 1760) of Cook Inlet volcanoes compiled by the Alaska Volcano Observatory (http://www.avo.alaska.edu/), and places such events in the context of regional Holocene volcanism.

2. Regional setting

Bear Lake is located in the Cook Inlet lowland, south-central Alaska (60° 25.20' N, 152° 21.40' W), 22 km southeast of Redoubt Volcano and ~3 km west of Cook Inlet (Fig. 1). Bear Lake has a surface area of 0.5 km^2 and a water volume of 4.9 km^3 (Fig. 2), and comprises two sub-basins, both with maximum depths of 17 m. The subbasins are separated by a 5-m-deep bathymetric high. The drainage-basin area is about 1.5 km^2 and the lake receives little input from surface inflow streams. A small stream exits the lake to the north. The land cover immediately surrounding Bear Lake is mostly shrub tundra. Alder arrived in the upper Cook Inlet region ca. 9500 cal yr, spruce arrived 1500 cal yr, and the modern vegetation assemblage was established soon after (Ager, 2000; Anderson et al., 2006), so terrestrial vegetative material has probably been deposited in the lake for most of the Holocene. The Cook Inlet lowlands were last glaciated during the late Wisconsin (Karlstrom, 1964; Reger and Pinney, 1996), and Bear Lake is a kettle formed in drift of this age. It is located 7 km northwest of the Harriet Point debris avalanche deposit originating from Redoubt Volcano of latest Pleistocene age described by Begét and Nye (1994). The present climate of the upper Cook Inlet region is transitional maritime continental. Spatial interpolation of climate-station data (Brabets et al., 1999) shows that the Bear Lake area has a mean annual temperature of about -3°C and mean annual precipitation of about 120 cm.

Five volcanoes of Quaternary age border the western Cook Inlet: Augustine, Hayes, Iliamna, Redoubt, and Spurr (Fig. 1). All have been active during the Holocene and are located within a radius of 130 km from Bear Lake. Bear Lake probably has received tephra from all five Cook Inlet volcanoes during the Holocene, although the majority of the tephras are likely from Redoubt Volcano, with its summit vent located only 22 km northwest of the lake. The most recent eruption at Redoubt Volcano occurred in AD 1989-1990 and consisted of multiple events from December 16 to April 26 (Scott and McGimsey, 1994). Other historical eruptions from Redoubt include AD 1902 and 1966-68 (Wallace et al., 2000).

The reported frequency of Holocene tephra fall for the Cook Inlet region ranges from about once every 100 yr (Begét et al., 1994; de Fontaine et al., in press) to once every 1000 yr (Riehle, 1985). Discrepancies in these records reflect the differential ability of various lakes or other depositional environments to record tephra fall, as well as their proximity to the major Cook Inlet volcanoes.

3. Methods

The bathymetry of Bear Lake was mapped prior to coring using a recording sonar fish-finder with integrated GPS. On the basis of the survey, multiple sites were targeted for coring (Fig. 2) in an attempt to recover the thickest sequence of lacustrine sediment. Cores were recovered in August 2005 with percussion and gravity corers operated from a floating platform. Three percussion (7.6 cm diameter) and companion surface cores (6.5 cm diameter), up to 5.6 and 0.7 m long, respectively, were taken from water depths ≤ 16 m. Coring at site BL-4 (Fig. 2), located on the interbasin bathymetric high, did not yield a percussion core. Core BL-3, along with its companion surface core, BL-3B (collectively, “BL-3/B”), contain the longest sedimentary sequence and are the focus of this paper.

One of the two surface cores from site BL-3 (core BL-3A) was extruded in contiguous 0.5 cm intervals, and the upper 8.5 cm were used for ^{210}Pb and ^{256}Cs dating. The other surface core BL-3B, was transported to the lab and used for tephra position and thickness measurements and correlation with the percussion core. Dry bulk density was measured on 4 cm^3 of sediment sampled from each 0.5 cm level. The activities of ^{137}Cs and ^{210}Pb (following subtraction of ^{226}Ra activity = excess ^{210}Pb, $^{210}Pb_{ex}$) were measured by gamma counting for a minimum of 2 days at the University of Southern California.

Laboratory analysis at Northern Arizona University was carried out in the following order: 1) cores were split, photographed, and the major physical sediment characteristics were described; 2) 1-2 cc of tephra was sieved at 1.0 mm (16 mesh) and the largest grain retained was measured with vernier calipers while the grain size of the representative bulk sample was visually compared with a standard grain size chart; 3) magnetic susceptibility (MS) was measured on split-core faces at 0.5 cm intervals using a Bartington MS2 meter with Surface Scanning Sensor MS2E; and 4) vegetation macrofossils for radiocarbon analysis were picked from sieved lake sediment, and dried under a laminar-flow hood. Samples were pre-treated using standard wet-chemistry techniques at University of Illinois, and analyzed for ^{14}C by AMS at Lawrence Livermore National Laboratory.

Twelve ^{14}C ages were obtained on terrestrial organic material (leaf blades and wood) from BL-3 (Table 2). Thin, black laminations are prominent and the core and contained leaves that were used for dating. The blade margin of a leaf from a depth of 284.5 cm below lake floor (blf) was identified as the genus *Alnus.* Other blade margins were not sufficiently preserved for identification but resembled sample BL-3-284.5. We attempted to date organic-rich layers near major tephra deposits to avoid long-distance extrapolation of their ages, while aiming for relatively even coverage across the core depth to facilitate a robust age-depth model. The ^{14}C ages were calibrated to calendar years using CALIB (v 5.0.2; Stuvier and Reimer, 1993). We used the median probability age output by CALIB as the single best estimate of the central tendency of the calibrated age (Telford et al., 2004b), and report all ages in reference to cal yr AD 1950.

4. Results

4.1. Core description

Sediment from Bear Lake includes two main types: organic-rich mud (gyttja) and tephra. Tephra comprises about 15% of the total thickness of the sediment sequence in core BL-3. Individual tephra layers range from 0.1 to 8.0 cm thick and most lack internal structure. Tephra grains are light to dark gray and range in size from ash to lapilli. Both glass shards and pumice fragments are present. On a fresh surface, the surrounding gyttja is olive-green to brown, but oxidizes rapidly to dark brown. Most of the tephra layers exhibit sharp basal contacts with the underlying gyttja and the upper contacts are gradational over a few millimeters (Fig. 3 photo inset). Comparison between measured MS and tephra layers shows that MS can be used to faithfully detect each tephra layer. A total of 67 tephra layers were documented in core BL-3/B; each tephra is labeled according to its basal depth measured to the nearest 1 mm blf (Table 3).

MS and lithological comparisons, as well as a 2nd-order polynomial ($r^2 \geq 0.999$) fit between visually correlated tephra of BL-3 and BL-3B (Fig. 3 graph inset) suggest that ~10 cm of sediment was lost during recovery of the percussion core. The non-linear depth correlation between the short and long cores from the same site is attributed to differential compaction during gravity and percussion coring. To account for the missing sediment, depths in core BL-3 were adjusted by 10.0 cm to obtain depths blf. The length of time for tephra deposition was considered to be negligible compared to the ambient sedimentation rate. As such, each tephra horizon was assigned an adjusted, tephra-free depth blf by subtracting the cumulative thickness of all overlying tephra.

4.2. Age model

4.2.1. ^{137}Cs and ^{210}Pb

^{210}Pb accumulates in lake sediments from natural, atmospheric fallout and decays to ^{226}Ra at a half life of 22.3 yr. ^{137}Cs was introduced into the atmosphere during nuclear weapons testing. Weapons testing, and subsequent ^{137}Cs fallout began in 1954 and peaked in 1963 (Wolfe et al., 2004). Accumulation rates determined from analyses of both isotopes provide independent dating techniques for sediment deposited during the last ~170 years. The ^{137}Cs profile rises from background levels at about 2.75 cm blf, then exhibits two peaks in the upper 2 cm blf (Fig. 4a). We correlate the initial rise with the onset of nuclear weapons testing ca. 1954 and the smaller peak (1.75 cm blf) with the height of atmospheric weapons testing in 1963. We tentatively correlate the highest value for ^{137}Cs activity at 0.75 cm blf with the Chernobyl nuclear reactor incident of 1986 which has been identified in lake sediments and glacier ice in the northern hemisphere (Pinglot and Pourchet, 1995). This interpretation yields an apparently constant sedimentation rate of about 0.4 mm yr^{-1} averaged over both the last ca. 20 and 40 yr, and about 0.5 mm yr^{-1} over the last 50 yr.

The $^{210}Pb_{ex}$ data were interpreted using the constant rate of supply (CRS) model (Appleby, 2001) to derive an age-depth curve for the top sediment (Fig. 4b). The CRS model assumes a constant flux of ^{210}Pb but accounts for the variable flux of sediment into the lake. It yields a weighted average sedimentation rate 0.06 cm yr^{-1} and a linear sedimentation rate of 0.07 cm yr^{-1} over the dated interval of 0 to 8.5 cm (Table 1; Fig. 4). These average rates agree with the interpretation of the data based on the constant initial ^{210}Pb concentration (CIC) model, which assumes a constant concentration of ^{210}Pb (not constant flux) at the lake surface. For this model, the logarithmic decrease of $^{210}Pb_{ex}$ activities plotted against depth yields a slope of -0.467 ± 0.053, resulting in an average sedimentation rate of 0.07 ± 0.01 cm yr^{-1}. The agreement lends further support for the CRS age model, which we use to assign ages to the tephras.

The CRS model indicates that sedimentation rate at site BL-3 is slightly higher than is indicated by the ^{137}Cs profile, resulting in age offsets of 10 to 20 yr. The coarse sampling interval and redistribution of the uppermost sediment may explain the observed age offset between ^{137}Cs and ^{210}Pb.

4.2.2. Integrated ^{210}Pb and ^{14}C

All 12 ^{14}C ages, the oldest age from the ^{210}Pb CRS model, and the modern (0 cm = 2005) were combined to construct an integrated age-depth model for core BL-3/B based on the tephra-free depths of the dated levels. We evaluated the performance of two functions in modeling the age-depth relation of the core: a least-squares polynomial and a cubic smooth spline (Fig. 5a). The latter was constructed using the formulation of Heegaard et al. (2005) and the statistical software R (http://cra.r-project/; last accessed 3 June 2006). For the least-squares fit, we chose a 4th-order polynomial because it is flexible enough to capture the major inflections in sedimentation rate ($r^2 = 0.999$), and because higher-order functions do not significantly improve the fit. For the spline fit, the stiffness of the curve is determined by the K value, which is the number of splines used in the regression. K values may range from 1 to n–1, where n = the number of dated levels. For K = n = 14, the age model (blue curve in Fig. 5a) appears to over-interpret changes in the sedimentation rate. Lower K values tend to produce a smoother fit, but show little difference between K = 3 and K = 13 for dated levels in BL-3/B. We selected K = 9, which is about the average of all model ages (3 < K < 14), determined by summing the absolute age difference of each 1 mm interval of each model versus the average of all models.

The 4th order least-squares and spline functions generate similar age-depth models for the core. The average absolute difference between the two models evaluated at 10 cm increments is 15 yr, and the two differ by more than 100 yr over only one short interval (440-400 cm; Fig. 5a inset). This similarity is despite the fact that the least-squares fit is based on the median probability age, whereas the spline fit uses the midpoint of the 1 sigma probability range. Where sedimentation-rate changes are more complicated, or where the number of ages is large relative to the number of sedimentation rate changes, then the spline function would likely out-perform other models (Telford et al., 2004a).

An additional advantage of the cubic spline model is its capability to estimate the age uncertainty at each level in the core (Heegaard et al., 2005). The model adopts a conservative approach to assessing the uncertainty by combining both the uncertainty associated with individual calibrated ages (within-object variation) with the uncertainty of how well the age represents the age of a particular core level (between-object variation). Following the Heegaard et al. (2005) formalisms, we used the 1 sigma calibrated age ranges for the ^{14}C ages as input to their error propagation function. For the one ^{210}Pb age, we assumed a conservative error of ± 20%. The error envelope output by the model encompasses the 2 sigma calibrated age range of nearly every individual ^{14}C age (Fig. 5b), and therefore seems appropriate. The resulting age uncertainty averages ± 105 yr over the ca. 8750 yr sediment sequence. For comparison, we also input the 2 sigma calibrated age ranges into the model, but found the resulting error envelope to be unrealistically broad over some segments of the core (Fig. 5b; average uncertainty = ± 140 yr). Following Heegaard et al. (2005), we adopt the error estimates derived using the 1 sigma calibrated ranges for tephras from Bear Lake (Table 3).

4.3. Tephra ages

The spline-fit age model shows that the core penetrated sediment as old as 8750 cal yr. The function generated a list of ages for each 1 mm increment of core, which we used to determine the age at the base of each of the 67 tephra layers (Table 3). On the basis of the spline-fit model, the average age uncertainty for the 67 tephras is the same as the average uncertainty over the entire core (± 105 yr).

We used the CRS model to assign ages to the top two tephras (BL-3B-3.0 and BL-3B-5.6). We recognize, however, that the position and thickness of these tephras was measured on a separate core (BL-3B) than that which was analyzed for ^{210}Pb and ^{137}Cs (BL-3A). We apply an uncertainty of ± 20% to approximate the error of applying the ^{210}Pb age from one core to the tephra in another. The ages of the two tephras are –15 ± 10 and 50 ± 20 cal yr (Fig. 4b), which suggests that they were derived from historical eruptions of Redoubt Volcano in AD 1966-68 and 1902 (Miller et al., 1998). Tephra from the most recent eruption of Redoubt Volcano (AD 1989-90) is not represented at Bear Lake, however, possibly because the eruption occurred in the winter months, when the surface of the lake was frozen, and because the predominant winter wind pattern is to the northeast. Similarly, sediment cores from Paradox and Tustemena lakes (Fig. 1) (de Fontaine, in press) on the Kenai Peninsula do not contain tephra from the 1989-90 eruption.

5. Discussion

5.1. Tephra-fall frequency

A histogram of tephra-fall frequency shows that the number of tephra layers preserved in Bear Lake sediment is not uniform throughout the Holocene (Fig. 6). Sediment deposited during the last 500 yr contains among the highest number of tephra layers (8) compared to other 500 yr intervals (average = 3.7 per 500 yr interval) back to 8500 cal yr. The Bear Lake sediment record shows extended periods (1000-2000 yr) of increased tephra-fall activity separated by shorter periods (500-1000 yr) of quiescence. Tephra-fall frequency was highest (n = 17) between ca 2000-3500, and lowest (n = 1) ca. 1000-1500 and 8000-8500 cal yr (Fig. 6).

Riehle (1985) presented data from a sediment core taken from the west sub-basin of Bear Lake in water depth of about 10 m (T. Ager, written communication, 2006), where sedimentation rate is lower compared to site BL-3 in the east sub-basin. Riehle's 2.8-m-long core spans at least 10,000 yr BP. Riehle (1985) characterized inter-tephra sediment as "silty fine sand," which was not found in core BL-3/B, suggesting that the shallower core site has a different sedimentation regime. This is supported by our surface core from site BL-4 in 5.5 m water depth, which contained a 6-cm-thick sand layer. Thirty-eight tephra layers were previously documented from Bear Lake by Riehle (1985). Based on grain size and geochemistry, 17 of the coarsest (pumice grain intermediate diameter >0.10 cm) tephra deposits were assigned to Redoubt Volcano, and 13 fine-grained tephras were provisionally assigned to Redoubt Volcano based on the assemblage of mafic phenocrysts. Thus, Riehle (1985) suggested that the average length of time separating Holocene eruptions of Redoubt Volcano was between 200 and 500 yr. No tephras were assigned to Iliamna, Spurr, or Augustine Volcanoes, at least one was correlated with Hayes volcano, and seven tephras could not be assigned to a source volcano.

Our core from Bear Lake contains almost twice the number of tephra layers over a shorter interval compared to Riehle's (1985) core from the same lake. We attribute the more complete record to a core site with higher sedimentation rate, and suggest that tephra layers from different eruptions might be amalgamated where sedimentation rates are lower. In addition, our core site is located in the center of the deepest sub-basin and farther from the shoreline, where bottom sediment is less likely to be remobilized by near-shore currents, especially if past lake levels were lower. All of the tephras are relatively pure and the sediment enclosing tephra layers contains little volcanic glass, indicated that each tephra is primary and that reworking of older tephra into younger deposits was minimal.

Using the same grain-size criterion as Riehle (1985), tephra layers containing grains of intermediate axis >0.10 cm was likely erupted from Redoubt Volcano. Twenty-nine tephras in our core meet this criterion (Table 3 bold), indicating an average tephra-fall frequency from Redoubt Volcano of once every 300 yr. This is an underestimate of the Redoubt Volcano eruption frequency because it does not include any of the finer-grained tephras, many of which were probably derived from Redoubt Volcano. Furthermore, we cannot account for tephra plumes that did not result in deposition at the bottom of Bear Lake (e.g., winter eruption of 1989-90). Our study of the provenance of Bear Lake tephras, including geochemical analyses, is in progress, and will provide a better estimate of the eruption frequency of Redoubt Volcano.

Wind patterns in the Cook Inlet region vary between seasons and modern wind patterns may not be representative of other times during the Holocene. Variations in tephra-fall frequency at Bear Lake, therefore, might reflect changes in wind patterns rather than changes in the eruptive activity. Plume height and short-term variations in wind direction also strongly influence tephra and ash-plume trajectory. For example, Scott and McGimsey (1994) report tephra distribution maps for the 1989-90 eruption that suggest highly variable wind patterns over the eruptive period, producing a wide area of thin, tephra deposits. With these considerations, the frequency of tephra fall determined from Bear Lake is considered a minimum.

5.2. Tephra correlations

Tephra BL-300.5 is most likely from the Hayes volcano, which produced the most widely distributed tephra of Holocene age yet identified in south-central Alaska (Riehle et al., 1990; Begét et al., 1991). The Hayes tephra is a set of multiple layers erupted between 3800 and 3500 ^{14}C yr BP (Riehle et al., 1990), which calibrates to between 4190 and 3780 cal yr. A distinguishing characteristic of the Hayes tephra is the presence of biotite phenocrysts (Riehle et al., 1990). In core BL-3/B, the fine-grained, 8-cm-thick tephra layer containing biotite comprises at least two tephra beds separated by 1.5 cm of brown gyttja with lower MS (Fig. 3). Our age model yields an age for the base of the tehpra set at 4030 ± 90 cal yr, within the range of previous estimates. Two other recently studied lake cores from Kenai Peninsula place the Hayes tephra between 3830 and 3730 cal yr (Paradox Lake) and between 4130 and 3780 cal yr (Tustumena Lake; Fig. 1) (de Fontaine et al., in press).

At least nine volcaniclastic deposits originating from Redoubt Volcano have been documented in the major valleys immediately surrounding the cone (Begét and Nye, 1994; Riehle et al., 1981). The largest deposit is located in the Redoubt Creek valley, 3 km south of Bear Lake and was emplaced about 10,500 ^{14}C yr BP, older than the base of our core. In the Crescent River valley, 20 km southwest of Bear Lake, another major eruption is represented by two clay-rich lahars dated at ca. 3600 ^{14}C yr BP (3965 to 3875 cal yr). ^{14}C ages from the outer ring of a large, in growth position tree constrains the age of these deposits (Begét and Nye, 1994). The only tephra within this age range in our core from Bear Lake is a 0.1-cm-thick, fine ash at 297.9 cm depth deposited 3930 ± 90 cal yr (Table 3). If this tephra layer was deposited during the same eruption that emplaced the lahars in Crescent River valley, then little tephra was produced or at least deposited at Bear Lake, despite the large lahars that were generated. Alternatively, there is a 3.5-cm thick ash at 275.5 cm depth, which is closely followed by a 1.2-cm-thick coarse ash dated at 3480 ± 90 cal yr. If the lahar deposits correlate with this tephra, then the age model from our core indicates an age of about 400 yr younger than the ^{14}C ages on wood buried by the lahars, which we cannot explain. The thick, coarse-ash could instead correlate with any of the two or three thick lahar deposits exposed along the North Fork of the Crescent River, where Begét and Nye (1994) describe evidence for series of small eruptions that generated lahars during the 2000 years following the emplacement of the voluminous Crescent River lahars. Twenty tephras from core BL3/B, of which nine have maximum grain size > 0.1 cm, fall within this time range, suggesting that the lahar record underestimates the number of eruptions of Redoubt Volcano.

Core BL3/B contains at least four tephras from Redoubt Volcano over the past 500 yr based on coarse grain size (Table 3, bold). This is consistent with the number of eruptions inferred from other evidence, including volcaniclastic deposits in the Drift River valley, north of Bear Lake (Begét and Nye, 1994), and the three tephras that were erupted from Redoubt Volcano within the past 500 yr and were identified in a core from Skilak Lake, located on the Kenai Peninsula, 150 km east of the Redoubt Volcano (Begét et al., 1994). The correlations between the tehpra at Bear Lake and any of these other deposits will require new geochemical analyses.

6. Conclusions

Lacustrine sediment from Bear Lake contains at least 67 tephra layers of Holocene age, at least 29 of which were likely erupted from nearby Redoubt Volcano. Our study reconfirms that lake deposits in south-central Alaska recovered by conventional coring techniques can yield high-quality records of tephra fall. It also provides an example of developing an age-depth model using a reasonable number of depth-controlled radiometric ages to determine the ages of many tephra layers. Our tephra record from the base of Redoubt Volcano nearly doubles the number of tephra-fall events at Bear Lake compared to previous studies and indicates an average fall frequency of one event every 300 yr. Our data also indicate extended periods of increased tephra fall between shorter periods of apparent quiescence, and adds a longer-term context to the volcano's historical activity (for example tephra-fall at Bear Lake during the past 500 yr was at least as frequent as any other 500 yr interval of the last 8500 yr). Our age-depth model also provides ages of tephra beds that can be used as time markers at other sites, and will be used as the basis for subsequent tephrochronology studies once geochemical analyses of the tephras are complete.

Acknowledgements

We thank Tom Ager (USGS) for sharing his knowledge of the original Bear Lake core and Chris Waythomas (USGS) for his continued encouragement. Chris Waythomas and Judy Fierstein (USGS) offered helpful suggestions on an earlier version. Feng Sheng Hu (UI) pretreated the vegetation macrofossils prior to AMS ^{14}C analysis. Vincent Todd (USC) assisted in the ^{210}Pb and ^{137}Cs analysis. This research was funded by the USGS/Alaska Volcano Observatory in coordination with NSF awards ATM-0318341 (DSK) and ATM-0317820 (AW). This work was performed, in part, under the auspices of the U.S. Department of Energy by University of California, Lawrence Livermore National Laboratory under Contract W-7405-Eng-48.

References

Anderson, R.S., Hallett, D.J., Berg, E., Jass, R.B., Toney, J.L., de Fontaine, C.S., DeVolder, A., 2006, Holocene development of boreal forest and fire regimes on the Kenai lowlands of Alaska. The Holocene 16, 791-803.

Andrews, J.T., Barber, D.C., Jennings, A.E., 1999. Errors in generating time-series and in dating events in late Quaternary millennial (radiocarbon) times-scales: Examples from Baffin bay, NW Labrador Sea, and east Greenland. In: Clark, P.U., Webb, R.S., Keigwin, L.D. (Eds.), Mechanisms of Global Climate Change at Millennial Time Scales. American Geophysical Union, Geophysical Monograph 112, pp. 23-34.

Appleby, P.G., 2001. Chronostratigraphic techniques in recent sediment. In: Last, W.M., Smol, J.P. (Eds.), Tracking Environmental Change Using Lake Sediments Volume 1: Basin Analysis, Coring, and Chronological Techniques. Kluwer, Dordrecht, The Netherlands, pp. 171-203.

Bennett, K.D., 1994. Confidence intervals for age estimates and deposition times in late-Quaternary sediment sequences. The Holocene 4, 337-348.

Brabets, T.P., Nelson, G.L., Dorava, J.M., Milner, A.M., 1999. Water-quality assessment of the Cook Inlet Basin, Alaska — Environmental setting. U.S. Geological Survey Water-Resources Investigations Report 99-4116, 110 p.

Begét, J.E., Nye, C.J., 1994. Postglacial eruption history of Redoubt Volcano, Alaska. Journal of Volcanology and Geothermal Research 62, 31-54.

Begét, J.E., Reger, R.D., Pinney, D., Gillispie, T., Campbell, K., 1991. Correlations of the Holocene Jarvis Creek, Tangle Lakes, Cantwell, and Hayes tephras in south-central Alaska. Quaternary Research 35, 174-189.

Begét, J.E., Stihler, S.D., Stone, D.B., 1994. A 500-year-long record of tephra falls from Redoubt Volcano and other volcanoes in upper Cook Inlet, Alaska. Journal of Volcanology and Geothermal Research 62, 55-67.

Boreux, J.-J., Pesti, G., Duckstein, L., Nacolas, J., 1997. Age model estimation in paleoclimatic research: fuzzy regression and radiocarbon uncertainties. Palaeogeography, Palaeoclimatology, Palaeoecology 128, 29-37.

de Fontaine, C.S., Kaufman, D.S., Anderson, R.S., Werner, A., Waythomas, C.F., Brown, T.A., in press. Late Quaternary distal tephra-fall deposits in lacustrine sediments, Kenai Peninsula, Alaska. Quaternary Research.

Heegaard, E., Birks, H.J.B., Telford, R.J., 2005. Relationships between calibrated ages and depth in stratigraphical sequences: an estimation procedure by mixed-effect regression. The Holocene 15, 612-618.

Karlstrom, T.N.V., 1964. Quaternary geology of the Kenai lowland and glacial history of the Cook Inlet region, Alaska. Geological Survey Professional Paper, 433, 69 p.

Miller, T.P., McGimsey, R.G., Richter, D.H., Riehle, J.R., Nye, C.J., Yount, M.E., and Dumoulin, J.A., 1998. Catalog of the historically active volcanoes of Alaska: U.S. Geological Survey Open-File Report OF 98-0582, 104 p.

Pinglot, J.F., Pourchet, M., 1995. Radioactivity measurements applied to glaciers and lake sediments. The Science of the Total Environment 173/174, 211-223.

Reger, R.D., Pinney, D.S., 1996. Late Wisconsin glaciation of the Cook Inlet region with emphasis on Kenai lowland and implications for early peopling. In: Davis, N.Y., Davis, W.E. (Eds.), The Anthropology of Cook Inlet: Proceedings from a Symposium. Cook Inlet Historical Society, Anchorage, pp. 5-23.

Riehle, J.R., 1985. A reconnaissance of the major Holocene tephra deposits in the upper Cook Inlet region, Alaska. Journal of Volcanology and Geothermal Research 26, 37-74.

Riehle, J.R., Kienle, J., Emmel, K.S., 198l. Lahars in Crescent River valley, lower Cook Inlet, Alaska. Alaska Division of Geological and Geophysical Surveys, Geological Report 53, 10 p.

Riehle, J.R., Bowers, P.M., Ager, T.A., 1990. The Hayes tephra deposits, an upper Holocene marker horizon in south-central Alaska. Quaternary Research 33, 276-290.

Scott, W., McGimsey, R., 1994. Character, mass, distribution, and origin of tephra-fall deposits of the 1989-1990 eruption of Redoubt Volcano, south-central Alaska. Journal of Volcanology and Geothermal Research 62, 251-272.

Stuvier, M., Polach, H.A., 1977. Discussion: Reporting of ^{14}C data. Radiocarbon 19, 355-363.

Stuvier, M., Reimer, P.J., 1993. Extended ^{14}C database and revised CALIB 3.0 ^{14}C calibration program. Radiocarbon 35, 215-230.

Telford, R.J., Heegaard, E., Birks, H.J.B., 2004a. All age-depth models are wrong, but how badly? Quaternary Science Reviews 23, 1-5.

Telford, R.J., Heegaard, E., Birks, H.J.B., 2004b. The intercept is a poor estimate of a calibrated radiocarbon age. The Holocene 14, 296-298.

Wallace, K.L., McGimsey, R.G., Miller, T.P., 2000. Historically active volcanoes in Alaska, a quick reference: U.S. Geological Survey Fact Sheet FS 0118-00, 2 p.

Wolfe, A.P., Miller, G.H., Olsen, C.E., Forman, S.L., Doran, P.T., Holmgren, S.U., 2004. Geochronology of high latitude lake sediments. In: Pienitz, R., Douglas, M.S.V., Smol, J.P. (Eds.), Long-term Environmental Change in Arctic and Antarctic Lakes. Kluwer, Dordrecht, The Netherlands, pp. 1-32.

Figure captions

Fig. 1. Location of Bear Lake and surrounding Cook Inlet volcanoes and other sites referenced in text. Historical eruptions (since AD 1760) are in parenthesis below the name of each volcano.

Fig. 2. (a) Redoubt Volcano and eastern lowlands to the Cook Inlet. (b) Bathymetric map of Bear Lake, showing core site locations.

Fig. 3. Lithostratigraphy of percussion core BL-3 and associated surface core BL-3B, with magnetic susceptibility (MS) profile and ^{14}C ages. Asterisks near MS measurement indicate measurements taken on tephra unintentionally extruded during core cutting. Equation 1 (graph inset) describes the depth relationship between tephra visually correlated between cores. Munsell soil colors were determined on a fresh surface and the color variations are shown in the stratigraphic log. Photo insert shows the two beds of the Hayes tephra, separated by 1.5 cm of light brown gyttja, a sharp, lower contact, and gradational upper contact.

Fig. 4. (a) Profiles of ^{137}Cs and $^{210}Pb_{ex}$ in surface core BL-3A, and (b) constant rate supply (CRS) and ^{14}C cubic-spline age models. Light gray bands with calendar years are assumed ages of three ^{137}C fallout events and dark gray bands indicate the assumed tephra locations, measured on core BL-3B. Ages of the two tephras are plotted where they intersect the CRS model (dashed line).

Fig. 5. (a) Comparison of age-depth models based on fits by a least-squares 4^{th}-order polynomial (red line) and cubic smooth spline (Heegaarrd et al., 2005), with K values = 9 (grey line) and 14 (blue line). Inset shows detail of interval where the departure of the two age-depth models is greatest. (b) Error envelopes output by the routine of Heegaard et al. (2005) based on input of both 1 and 2 sigma age ranges. Each tephra in core BL-3/B was assigned an age based on the spline fit with K = 7; associated age uncertainties were based on error estimates that incorporate the 1 sigma age ranges. Individual ^{14}C ages are shown as calibrated median probability age with errors of 2 sigma ranges output by CALIB (Table 2).

Fig. 6. Histogram showing the frequency distribution of tephra ages in Bear Lake sediment.

Figure 1

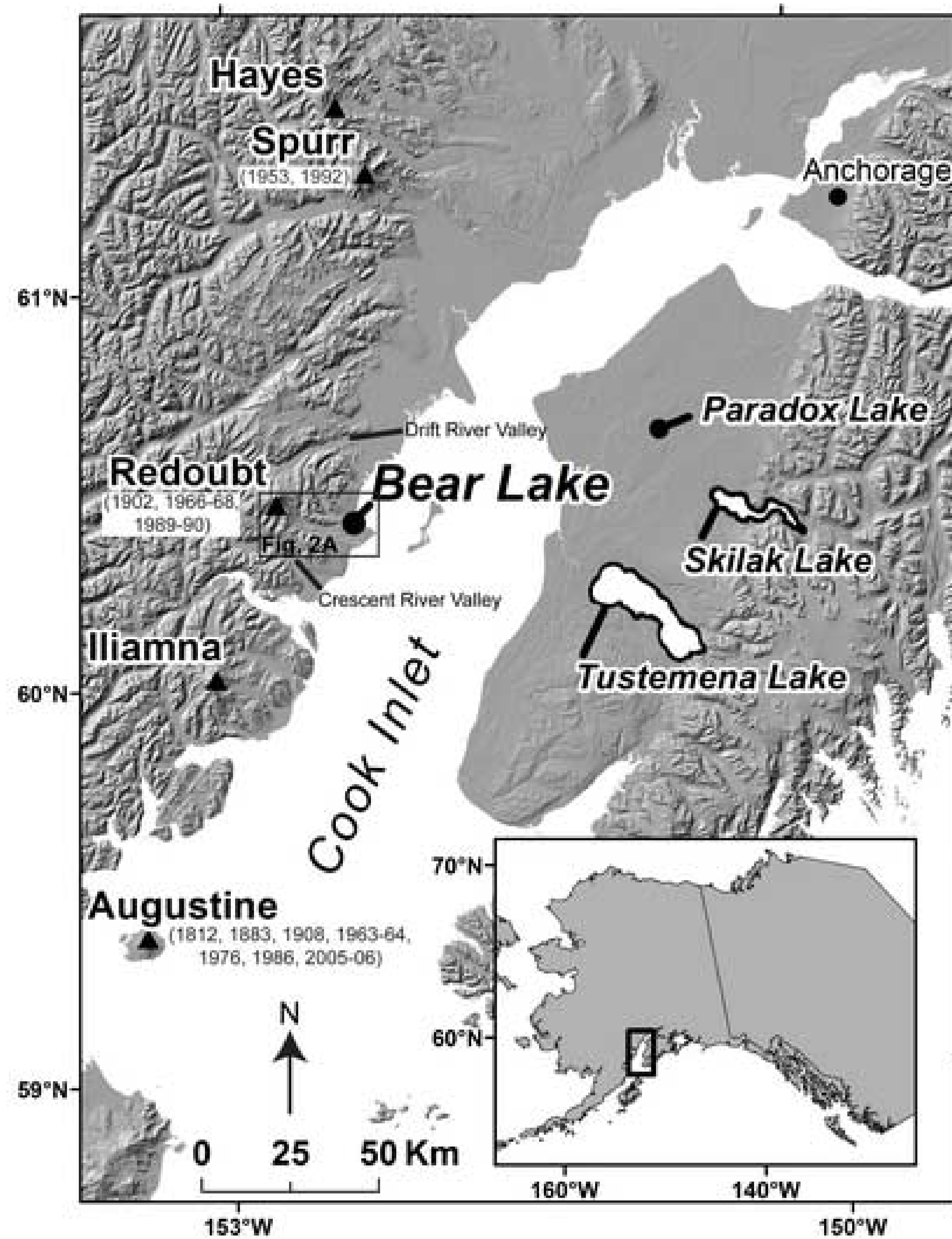

Hayes
Spurr
(1953, 1992)
Anchorage
61°N
Paradox Lake
Drift River Valley
Redoubt
(1902, 1966-68, 1989-90)
Bear Lake
Fig. 2A
Skilak Lake
Crescent River Valley
Iliamna
Tustemena Lake
60°N
Cook Inlet
Augustine
(1812, 1883, 1908, 1963-64, 1976, 1986, 2005-06)
70°N
60°N
N
59°N
0 25 50 Km
160°W
140°W
153°W
150°W

Figure 2

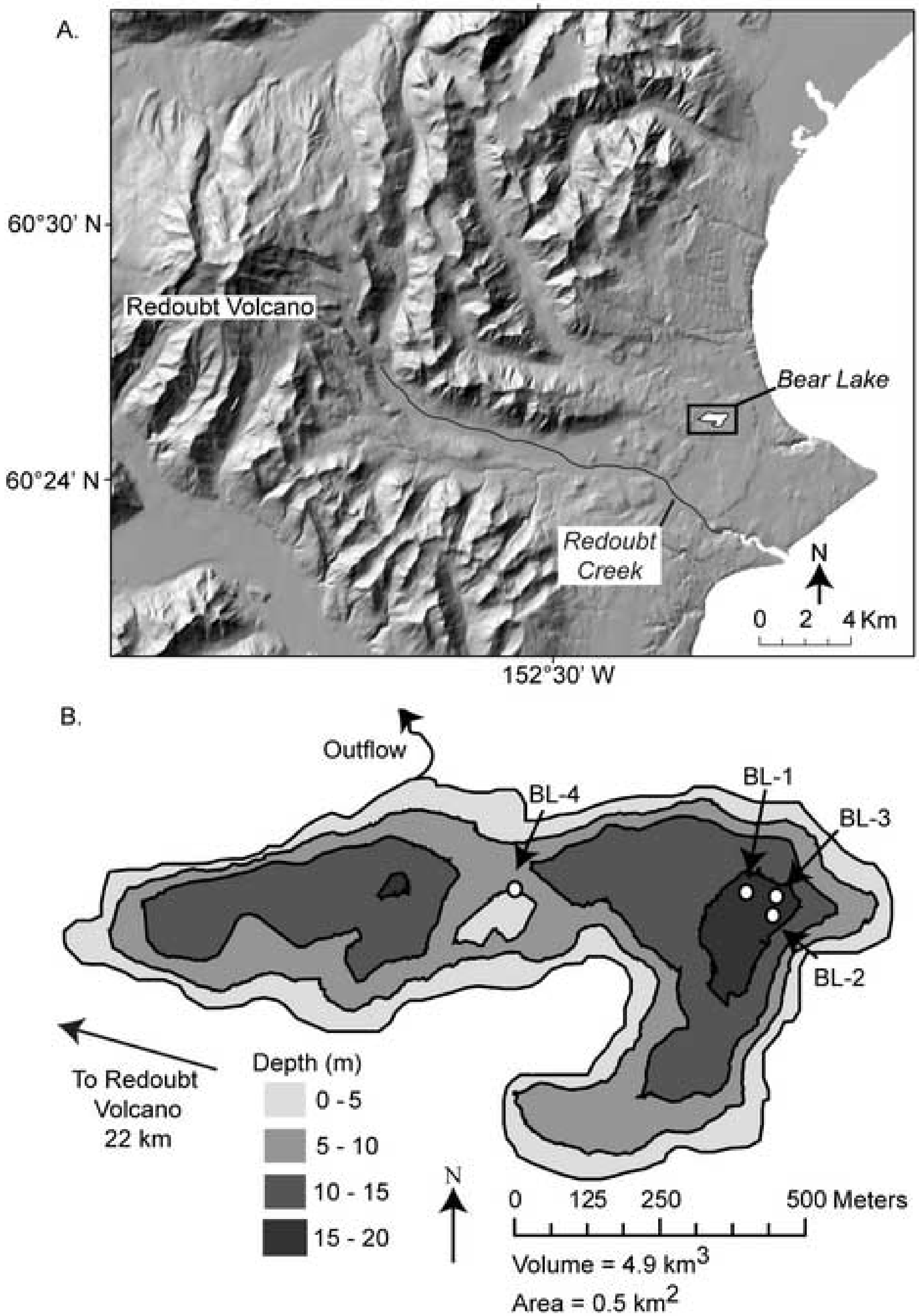
A.
60°30' N
60°24' N
152°30' W
Redoubt Volcano
Bear Lake
Redoubt
Creek
N
0 2 4 Km
B.
Outflow
BL-4
BL-1
BL-3
BL-2
To Redoubt
Volcano
22 km
Depth (m)
0 - 5
5 - 10
10 - 15
15 - 20
N
0 125 250 500 Meters
Volume = 4.9 km3
Area = 0.5 km2

Figure 3

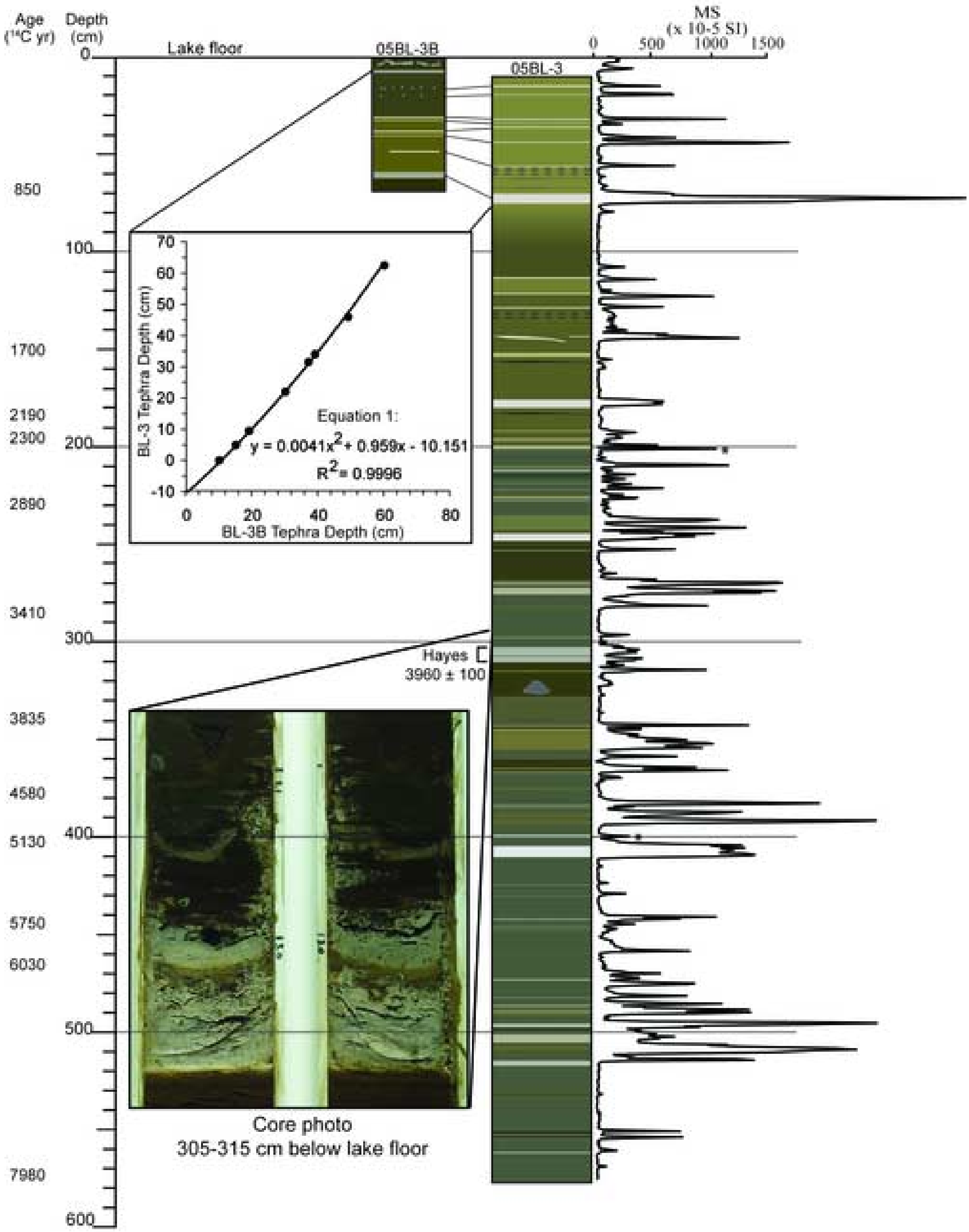

Age (^{14}C yr)
Depth (cm)
Lake floor
05BL-3B
05BL-3
MS (x 10-5 SI)
0 500 1000 1500
850
1700
2190
2300
2890
3410
3835
4580
5130
5750
6030
7980
0
100
200
300
400
500
600
BL-3 Tephra Depth (cm)
BL-3B Tephra Depth (cm)
Equation 1:
$y = 0.0041x^2 + 0.959x - 10.151$
$R^2 = 0.9996$
Hayes
3960 ± 100
Core photo
305-315 cm below lake floor

Figure 4

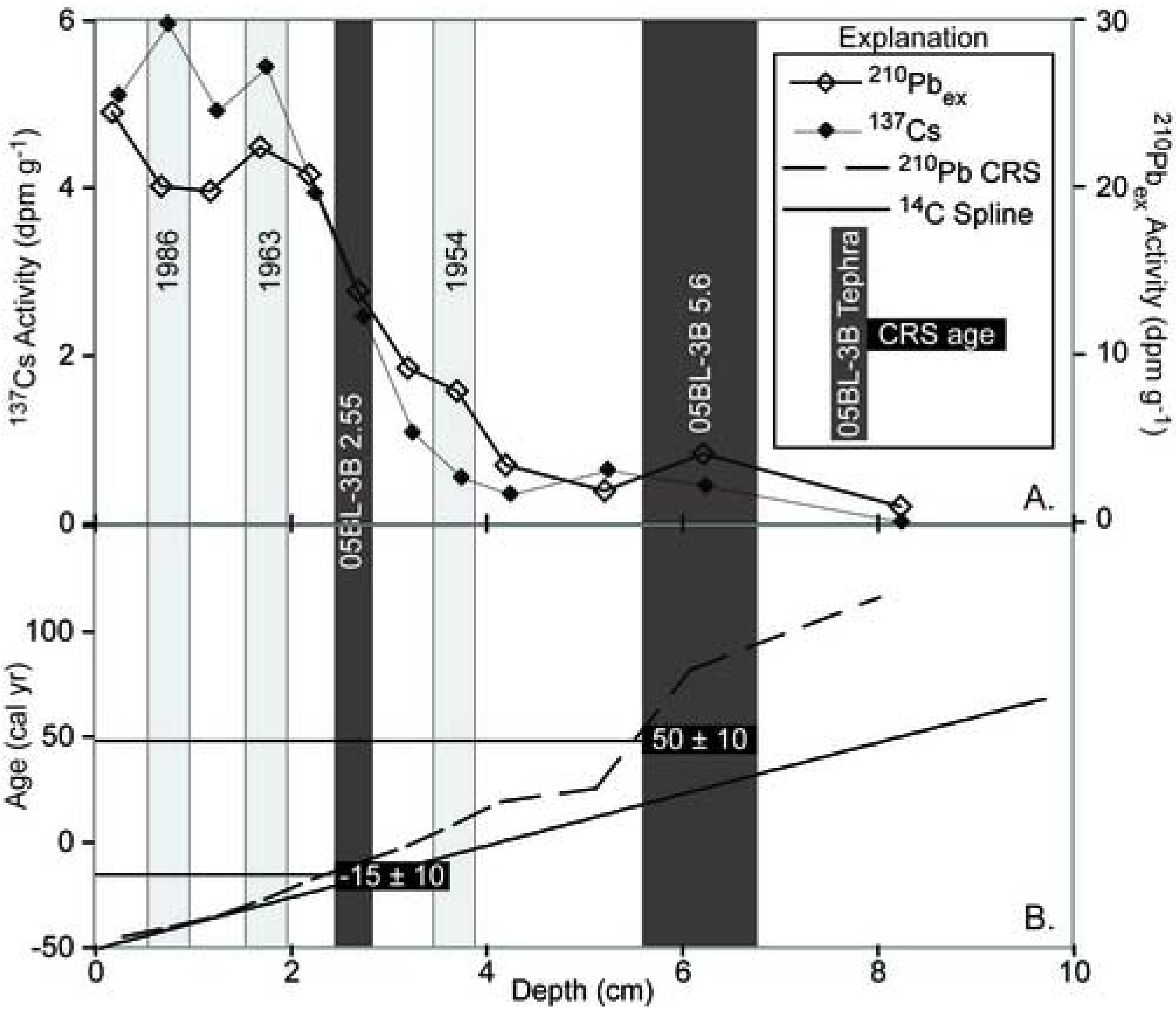

Explanation
$^{210}Pb_{ex}$
^{137}Cs
^{210}Pb CRS
^{14}C Spline
05BL-3B Tephra
CRS age
1986
1963
1954
05BL-3B 2.55
05BL-3B 5.6
50 ± 10
-15 ± 10
A.
B.
^{137}Cs Activity (dpm g^{-1})
$^{210}Pb_{ex}$ Activity (dpm g^{-1})
Age (cal yr)
Depth (cm)

Figure 5

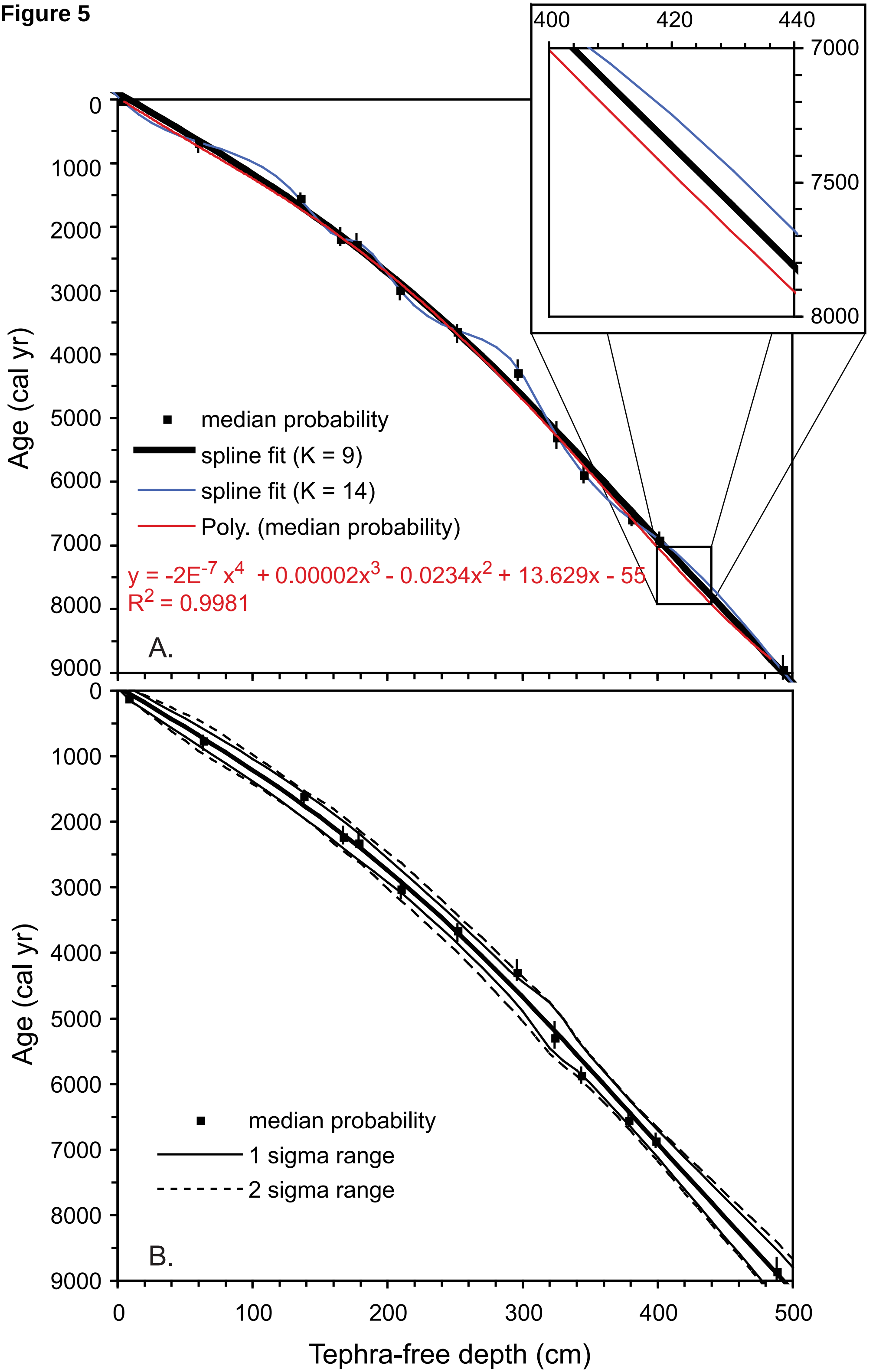

400
420
440
7000
7500
8000
0
1000
2000
3000
4000
5000
6000
7000
8000
9000
Age (cal yr)
median probability
spline fit (K = 9)
spline fit (K = 14)
Poly. (median probability)
y = -2E-7 x4 + 0.00002x3 - 0.0234x2 + 13.629x - 55
R2 = 0.9981
A.
median probability
1 sigma range
2 sigma range
B.
0
100
200
300
400
500
Tephra-free depth (cm)

Figure 6

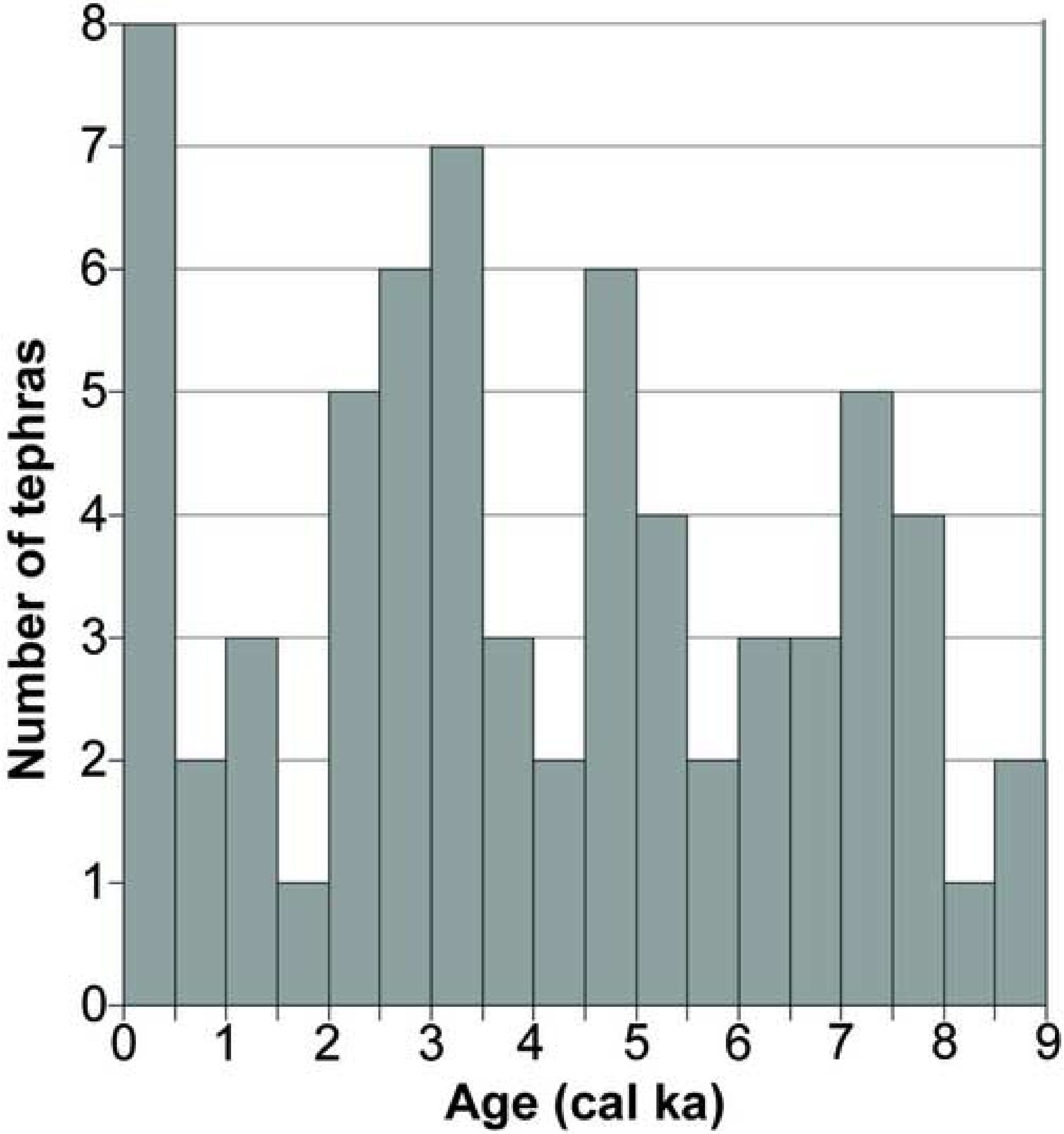

Table 1

Table 1

^{210}Pb, ^{226}Ra, and ^{137}Cs activity, core BL-3A, and calculated $^{210}Pb_{ex}$ inventory and constant rate of supply model ages (relative to AD 1950)

Depth (cm blf)	Density (g cm^{-3})	^{210}Pb (dpm g^{-1})		^{226}Ra (dpm g^{-1})		^{137}Cs (dpm g^{-1})		$^{210}Pb_{ex}$ (dpm cm^{-2})	Age (yr)[a]
0-0.5	0.22	24.78	± 1.42	0.32	± 0.18	5.10	± 0.21	2.69	-49
0.5-1.0	0.20	20.35	± 1.05	0.36	± 0.14	5.95	± 0.16	2.00	-45
1.0-1.5	0.20	20.22	± 1.27	0.52	± 0.06	4.91	± 0.19	1.97	-39
1.5-2.0	0.20	22.37	± 1.43	0.00	± 0.21	5.44	± 0.22	2.24	-31
2.0-2.5	0.21	21.32	± 1.14	0.61	± 0.16	3.93	± 0.16	2.18	-21
2.5-3.0	0.19	13.69	± 1.33	0.05	± 0.21	2.45	± 0.22	1.30	-13
3.0-3.5	0.22	9.19	± 1.16	0.19	± 0.17	1.07	± 0.15	0.99	-5
3.5-4.0	0.26	8.05	± 0.86	0.42	± 0.13	0.54	± 0.11	0.99	6
4.0-4.5	0.32	3.74	± 0.93	0.58	± 0.13	0.34	± 0.11	0.76	17
5.0-5.5	0.19	1.88	± 1.45	0.25	± 0.21	0.63	± 0.16	0.31	23
6.0-6.5	0.21	3.92	± 1.30	0.09	± 0.17	0.44	± 0.14	1.21	82
8.0-8.5	0.18	0.69	± 1.34	0.01	± 0.23	0.01	± 0.17	0.15	117

[a]Age relative to AD 1950 estimated from measured excess ^{210}Pb, bulk density, and sample-interval thickness. Interpolated thicknesses were used for the four deepest samples.

Table 2

Table 2

Radiocarbon ages from core BL-3

Depth (cm blf)[a]	Tephra-free depth (cm)[a]	Lab ID (CAMS-)	^{14}C age (yr BP)	Calibrated age (cal yr)[b]	Dated material
67.5	63.4	120731	850 ± 35	780 ± 46	Leaf blades
150.0	137.8	120732	1705 ± 35	1612 ± 70	Leaf blades
183.0	166.8	120733	2185 ± 35	2230 ± 80	Leaf blades
195.0	178.4	120734	2300 ± 40	2320 ± 80	Leaf blades
229.5	209.8	120735	2890 ± 35	3030 ± 60	Wood
284.5	251.6	120736	3410 ± 35	3660 ± 50	*Alnus* leaf blades
339.5	295.5	120737	3835 ± 35	4290 ± 70	Leaf blades
377.5	323.8	120738	4575 ± 35	5290 ± 180	Leaf blades
402.0	343.4	120875	5125 ± 35	5870 ± 80	Leaf blades
444.0	378.4	120876	5720 ± 35	6550 ± 70	Leaf blades
465.0	398.6	120877	6025 ± 35	6870 ± 70	Leaf blades
572.5	488.1	120878	7980 ± 40	8860 ± 100	Leaf blades

Note: ^{14}C ages were calculated following the conventions of Stuiver and Polach (1977) including assumed $\delta^{13}C$ values of -25‰.

[a]Centered depth of sampled layer.

[b]Median probability ± one half of 1 σ age range from CALIB v.5.0.2 (Stuvier and Reimer, 1993).

Table 3

Table 3

Tephra depth, thickness, median and maximum grain size, and age, core BL-3/B

Tube depth (cm)[a]	Depth (cm blf)[a]	Thickness (cm)	Grain size	Max grain size (cm)[b]	Modeled Tephra age (cal yr BP)[c]
3.0[d]	3.0	0.4	fine ash	0.5	-15 ± 10
7.5[d]	**7.5**	**1.5**	**fine ash**	**3.0**	**50 ± 20**
5.2	**15.2**	**0.6**	**fine ash**	**2.0**	**100 ± 50**
9.2	**19.2**	**0.2**	**coarse ash**	**1.5**	**150 ± 50**
22.2	32.2	0.4	fine ash	0.5	300 ± 60
24.3	34.3	0.1	fine ash	0.3	330 ± 60
31.4	41.4	0.3	fine ash	0.5	410 ± 60
34.4	**44.4**	**0.4**	**fine ash**	**1.0**	**440 ± 60**
46.1	**56.1**	**0.2**	**fine ash**	**6.0**	**590 ± 70**
65.0	**75.0**	**5.2**	**fine ash**	**3.0**	**760 ± 80**
104.4	114.4	0.4	fine ash	0.5	1270 ± 90
113.3	**123.3**	**1.2**	**coarse ash**	**6.0**	**1380 ± 90**
118.5	**128.5**	**0.2**	**coarse ash**	**3.5**	**1450 ± 90**
134.1	**144.1**	**1.1**	**fine ash**	**1.0**	**1660 ± 100**
169.5	**179.5**	**4.0**	**medium lapillus**	**10.0**	**2130 ± 100**
185.9	**195.9**	**0.4**	**fine ash**	**2.5**	**2390 ± 110**
187.1	197.1	0.1	fine ash	0.3	2410 ± 100
190.5	**200.5**	**1.1**	**fine ash**	**1.0**	**2450 ± 100**
192.0	202.0	0.5	fine ash	0.5	2460 ± 100
200.4	**210.4**	**0.6**	**fine ash**	**1.5**	**2600 ± 100**
202.8	212.8	0.6	fine ash	0.3	2630 ± 100
205.1	215.1	0.1	fine ash	0.3	2660 ± 90
209.1	219.1	0.1	fine ash	0.3	2730 ± 90
212.0	**222.0**	**0.3**	**fine ash**	**3.5**	**2780 ± 90**
217.2	227.2	0.2	fine ash	0.3	2860 ± 90
228.4	238.4	1.8	fine ash	0.3	3030 ± 90
233.0	243.0	1.8	fine ash	0.5	3080 ± 90
239.5	**249.5**	**4.0**	**fine lapillus**	**9.0**	**3120 ± 90**
243.1	**253.1**	**0.3**	**fine ash**	**2.5**	**3180 ± 90**
258.4	268.4	0.3	fine ash	0.3	3460 ± 90
260.6	**270.6**	**1.2**	**coarse ash**	**2.0**	**3480 ± 90**
265.5	275.5	3.5	fine ash	0.3	3510 ± 90
271.8	281.8	0.3	fine ash	0.5	3620 ± 90
287.9	297.9	0.1	fine ash	0.3	3930 ± 90
300.5[f]	310.5	8.0	fine ash	0.3	4030 ± 90
305.2	315.2	0.7	fine ash	0.3	4110 ± 90

312.8	322.8	2.3	fine ash	0.3	4210 ± 90
333.6	343.6	0.6	coarse ash	0.5	4640 ± 110
335.2	345.2	0.4	fine ash	0.3	4660 ± 110
345.0	**355.0**	**7.4**	**medium lapillus**	**210.0**	**4710 ± 120**
349.6	359.6	0.2	fine ash	0.3	4810 ± 130
355.0	365.0	0.5	fine ash	0.3	4920 ± 150
356.8	366.8	0.6	coarse ash	0.5	4940 ± 150
374.0	**384.0**	**0.6**	**fine ash**	**2.0**	**5310 ± 170**
376.1	386.1	0.1	fine ash	0.3	5360 ± 160
379.5	**389.5**	**1.7**	**medium lapillus**	**7.0**	**5400 ± 150**
383.5	**393.5**	**2.5**	**fine ash**	**1.5**	**5430 ± 140**
390.0	400.0	?[g]	?[g]	0.3	5580 ± 120
400.8	**410.8**	**6.3**	**coarse ash**	**2.5**	**5680 ± 110**
414.4	424.4	0.1	fine ash	0.3	5980 ± 100
420.1	430.1	0.1	fine ash	0.3	6110 ± 100
432.3	**442.3**	**0.5**	**coarse ash**	**1.5**	**6370 ± 100**
435.8	445.8	0.3	fine ash	0.2	6450 ± 100
438.4	448.4	0.2	fine ash	0.3	6500 ± 100
449.5	459.5	0.3	fine ash	0.3	6740 ± 100
463.3	**473.3**	**0.7**	**coarse ash**	**2.5**	**7040 ± 110**
472.4	482.4	0.2	fine ash	0.5	7240 ± 120
476.9	486.9	1.1	fine ash	0.5	7320 ± 120
480.0	**490.0**	**1.7**	**fine lapillus**	**3.5**	**7350 ± 120**
481.8	491.8	1.5	fine ash	0.3	7360 ± 120
487.2	497.2	1.4	fine ash	0.5	7450 ± 130
495.2	**505.2**	**4.2**	**medium lapillus**	**14.0**	**7530 ± 130**
501.4	**511.4**	**4.8**	**coarse ash**	**4.0**	**7560 ± 130**
505.7	515.7	0.8	fine ash	0.5	7640 ± 140
542.3	**552.3**	**0.3**	**fine ash**	**1.0**	**8460 ± 170**
545.0	**555.0**	**0.2**	**fine ash**	**2.0**	**8510 ± 170**
552.0	562.0	0.6	fine ash	0.5	8660 ± 180

Note: Bold = tephras with maximum grain size > 1.0 mm; probably originating from Redoubt Volcano (Riehle, 1985).

[a]Depth below lake floor (blf) to base of tephra.

[b]Long axis of the largest single grain for tephras with grains > 1.0 mm. Otherwise, maximum grain size was categorized for intervals of 0.3, 0.5, and 1.0 mm.

[c]Age and age uncertainties based on model shown in Fig. 5.

[d]Tephras recovered from surface core BL-3B.

[e]Ages based on ^{210}Pb constant rate of supply (CRS) age model (Fig. 4b) with assumed ±20% uncertainty.

[f]Presence of biotite is inferred to be diagnostic of the Hayes tephra.

[g]Tephra located at core break and thickness could not be ascertained.